Published in final edited form as:
Stem Cells Dev. 2011 November ; 20(11): 1817–1827. doi:10.1089/scd.2011.0042.

Isolation and Characterization of Node/Notochord-Like Cells from Mouse Embryonic Stem Cells

Maria K. Winzi[1], **Poul Hyttel**[2], **Jacqueline Kim Dale**[3], and **Palle Serup**[1]

[1]Department of Stem Cell Biology, Hagedorn Research Institute, Gentofte, Denmark

[2]Department of Basic Animal and Veterinary Sciences, Faculty of Life Sciences, University of Copenhagen, Frederiksberg C, Denmark

[3]Division of Cell and Developmental Biology, College of Life Sciences, University of Dundee, Dundee, United Kingdom

Abstract

The homeobox gene *Noto* is expressed in the node and its derivative the notochord. Here we use a targeted *Noto*-GFP reporter to isolate and characterize node/notochord-like cells derived from mouse embryonic stem cells. We find very few *Noto*-expressing cells after spontaneous differentiation. However, the number of *Noto*-expressing cells was increased when using Activin A to induce a *Foxa2*- and *Brachyury*-expressing progenitor population, whose further differentiation into *Noto*-expressing cells was improved by simultaneous inhibition of BMP, Wnt, and retinoic acid signaling. Noto-GFP$^+$ cells expressed the node/notochord markers *Noto, Foxa2, Shh, Noggin, Chordin, Foxj1*, and *Brachyury*; showed a vacuolarization characteristic of notochord cells; and can integrate into midline structures when grafted into Hensen's node of gastrulating chicken embryos. The ability to generate node/notochord-like cells in vitro will aid the biochemical characterization of these developmentally important structures.

Introduction

Spemann and Mangold discovered that newt dorsal blastoporal lips (Spemann's organizer) can induce a secondary body axis when grafted to a host embryo [1]. Equivalent organizers are found in other species like chicken (Hensen's node) and mouse. The mouse node arises from the anterior end of the primitive streak (PS) at the mid-to-late streak stages. At embryonic day (E) 7.5 the pit of the node has formed and the final shape is established. Node cells have a small apical surface with a monocilium, which plays a role in establishing the left-right asymmetry in the embryo [2-4]. The node is the precursor of midline structures, including floor plate and notochord [5]. Numerous studies have shown that the notochord plays a critical role in patterning of surrounding tissues [6-10]. Formation of the node depends on Nodal signaling [11] and is regulated by the transcription factors Foxa2, Brachyury (T), and Noto [12-16]. Foxa2 null embryos fail to form the node and notochord [14], whereas T and Noto are crucial for development of the trunk and tail notochord [16,17]. Furthermore, Noto is required to maintain axial mesoderm identity most likely by inhibition of paraxial mesoderm fate [16]. *Noto* and its orthologs [*Xnot* in Xenopus, *floating*

Address correspondence to: Dr. Palle Serup, Department of Stem Cell Biology, Hagedorn Research Institute, Niels Steensens Vej 6, DK-2820 Gentofte, Denmark, pas@hagedorn.dk.

Author Disclosure Statement
No competing financial interests exist.

Europe PMC Funders Author Manuscripts

head (*flh*) in zebrafish and *Gnot1*/*Gnot2* in chicken] show similar expression patterns in the notochord and are important markers to study notochord induction. Zebrafish studies demonstrated that low concentrations of the Nodal homologs cyclops and squint are essential for *flh* induction, whereas high concentrations favor *goosecoid* (*gsc*) expression [18,19]. In Xenopus, Activin and Fgf may act as inducers of *Xnot* [20]. Additionally, the nodalrelated factor Xnr1 can together with Noggin induce a complete secondary axis [21], whereas co-repression of BMP4 and Wnt signaling is required for specification of the notochord [22]. Retinoic acid (RA) may activate Gnot1 expression in the chicken [23]. Notch signaling is also involved in midline specification from organizer precursors where activation of the Delta-Notch pathway favors a floor plate fate and inhibits contribution to the notochord [24-29]. Mouse embryonic stem (ES) cells are excellent tools to study development in vitro and reporter cell lines have served to monitor differentiation into all 3 germ layers. Directed differentiation of ES cells into rare cell types, for example, node and notochord cells, can provide access to large numbers of such cells and thus facilitate biochemical characterization of these. In this study we take advantage of an eGFP reporter targeted to the *Noto* locus [12,16] to study node and notochord formation in vitro. We show that formation of Noto-expressing cells is augmented when a $Foxa2^{+}T^{+}$ double positive progenitor population is first induced by a low concentration of Activin A. Further differentiation toward a Noto-expressing fate is promoted by the simultaneous inhibition of endogenous RA, BMP and Wnt signaling and the presence of Fgf2. In vitro derived Noto-GFP^{+} cells share marker expression and morphology with node and notochord cells in vivo.

Materials and Methods

Cell culture of $Noto^{Gfp/+}$ and $T^{Gfp/+}$ cells

Noto$^{Gfp/+}$ and *T*$^{Gfp/+}$ mouse ES cells were described previously [12,30]. Mouse ES cells were maintained in serum- and feeder-free cultures in the presence of BMP4 + LIF [31] or 2i + LIF [32]. To initiate differentiation cells were seeded at 2,000–4,000 cells/cm^2 on gelatin-coated plastic ware (Nunc) in KO-DMEM supplemented with N2, B27, 0.1 mM nonessential amino acids, 2 mM L-glutamine, Penicillin/Streptomycin (all from Invitrogen), and 0.1 mM 2-mercaptoethanol (Sigma Aldrich). The following growth factors and small molecule compounds were used: Activin A, Wnt3a, Nodal, BMP4, Noggin, Dkk1, Shh (all from R&D Systems), and Fgf2 (Invitrogen), SB431542 [33], SU5402 (Calbiochem), and AGN193109 (synthesized by Novo Nordisk A/S) [34]. The total number of cells was determined by the NucleoCounter (Chemometec A/S).

Transfection of Noto-GFP cells

At day 2 of differentiation *Noto*$^{Gfp/+}$ cells were transfected with plasmid DNA using Lipofectamine2000 (Invitrogen) according to the manufacturer's protocol.

Flow cytometry

The FACScalibur (BD Biosciences) flow cytometer was used for analytical quantification of GFP^{+} cells in at least 3 independent experiments. Sorting of Noto-GFP^{+} cells for RNA extraction was performed on a FACSAria (BD Biosciences).

Quantitative real-time reverse transcriptase–polymerase chain reaction

The extraction of the total RNA with the Invisorb Spin Cell RNA Mini kit (Invitek) was done according to the manufacturer's instructions. cDNA was prepared from 100 ng RNA using MMLV Reverse Transcriptase (Invitrogen). Quantitative real-time reverse transcriptase-polymerase chain reaction (qRT-PCR) was performed using Brilliant® SYBR® Green QPCR Master Mix (Stratagene) and the standard SYBR Green program with

dissociation curve of the Mx3005P (Stratagene). Quantified values for each gene were normalized against the housekeeping gene *G6pdh*. The results are expressed as the relative expression level compared with the expression in undifferentiated cells. For primer sequences see Supplementary Table S1 (Supplementary Data are available online at www.liebertonline.com/scd).

Immunocytochemistry

Immunocytochemistry (ICC) was done as described previously [35]. The following antibodies were used: goat anti-Foxa2 (Santa Cruz Biotechnology), goat anti-T (R&D Systems), rat anti-Flk1 (BD Pharmingen), goat anti-Sox17 (R&D Systems), Alexa 488 conjugated rabbit anti-GFP (Molecular Probes/Invitrogen), and goat anti-Shh (R&D Systems). The cells were incubated with Cy2-, Cy3-, or Cy5-conjugated species-specific secondary antibodies (Jackson Immuno-Research Laboratories) and 4′,6-diamidino-2-phenylindole (MP Biomedicals). The slides were analyzed using an LSM 510 META laser scanning microscope (Carl Zeiss).

EdU incorporation

Noto-GFP ES cells were differentiated with or without Fgf2 in step 2. At day 5 EdU (Invitrogen) was added directly to the medium resulting in a final concentration of 10 μM. After 15 min of incubation cells were fixed in 4% formaldehyde solution for 15 min at RT. EdU staining was performed according to the manufacturer's instructions using Alexa 594 as fluorescent dye. EdU staining was followed by ICC against GFP as described above. The slides were analyzed using an LSM 510 META laser scanning microscope (Carl Zeiss). In 3 independent experiments between 40 and 46 GFP^+ cell clusters for each condition were documented and within each GFP^+ cell cluster the number of GFP^+ and EdU^+ cells were counted manually.

Transmission electron microscopy

Clumps of Noto-GFP^+ cells were manually scraped off the culture dish and fixed in 3% glutaraldehyde in 0.1 M sodium phosphate buffer (pH 7.2) for 1 h at 4 °C. Dehydration, embedding in Epon, and sectioning was done as described previously [36]. Transmission electron microscopy was performed on a Phillips CM100 transmission electron microscope, and digital image processing was applied.

Hensen's node grafting in chicken embryos

Fertilized eggs from white leghorn chicken were purchased from Triova and incubated at 39 °C in a humidified incubator. Node grafting at Hamburger and Hamilton stage (HH st) 4 chicken embryos was done as described previously [29]. Grafting lateral to the neural tube was done in early chick cultures at HH st 8–10 [37]. Clumps of Noto-GFP^+ cells were scraped off, labeled with fluorescent CellTracker™ Orange CMTMR dye (Molecular Probes/Invitrogen), and grafted into chicken embryos. After 20–48 h the embryos were isolated, fixed in 4% PFA, and stored in methanol at −20 °C for further staining. Whole-mount immunofluorescent analyses of manipulated chicken embryos were performed as previously described [38]. The following antibodies were used: goat anti-Foxa2 (Santa Cruz Biotechnology) and Alexa 488 conjugated rabbit anti-GFP (Molecular Probes/Invitrogen). Embryos were embedded into 4% agar for vibratome sectioning.

Statistics

Mean% GFP^+ cells [fluorescence-activated cell sorting (FACS)] ± standard deviation or mean relative expression (qRT-PCR) ± standard error of the mean was calculated and statistical analyses were performed using a 2-tailed Student's *t*-test.

Results

Induction of a Noto-GFP$^+$ population via a Foxa2$^+$T$^+$ precursor population

We first examined the influence of Activin A/nodal signaling on the differentiation of *Noto*$^{Gfp/+}$ cells when grown in adherent culture in serum- and feeder-free medium. Approximately 1% of the cells activated GFP expression spontaneously after 5 days of differentiation and addition of Activin A in various concentrations did not increase the number of Noto-GFP$^+$ cells above that observed during spontaneous differentiation (Fig. 1A). Increasing the concentration of Activin A above 1 ng/mL had an inhibitory effect on the number of Noto-GFP$^+$ cells, and a similar effect was seen using high concentrations of Nodal (Fig. 1A, B). Previous observations in Xenopus demonstrated that inhibition of BMP and Wnt signaling is required for notochord development [20,22] and that Fgf signaling can induce *Xnot* expression [20]. These observations led us to test the influence of Wnt, BMP, and Fgf signaling upon differentiation of *Noto*$^{Gfp/+}$ cells. We found that BMP4 suppressed the induction of Noto-GFP$^+$ cells ($P < 0.05$) and that the inhibitory effect was reversed by adding the BMP antagonist Noggin. Nevertheless, inhibition of endogenous BMP signaling by Noggin was not able to increase the differentiation into Noto-GFP$^+$ cells (Fig. 1C). Stimulation or inhibition of Wnt and Fgf signaling alone did not change Noto-GFP expression (Fig. 1D, E).

Since the node develops from a Foxa2$^+$T$^+$ population in the anterior PS and mouse knock-out studies have shown that *Noto* expression is completely lost in Foxa2 and T null embryos [12], we devised a differentiation protocol to induce a Foxa2 and T double-positive cell population before attempting to differentiate such cells further to a Noto$^+$ stage. Low concentrations of Activin A are known to induce T expression in mouse ES cells, whereas high Activin A concentrations inhibit T induction [35]. We therefore used a *T*$^{Gfp/+}$ reporter mouse ES cell line to titrate the Activin A concentration that resulted in the highest number of T-GFP$^+$ cells as assayed by FACS analysis. We found that 1 ng/mL Activin A present for 4 days yielded in the highest induction of T-GFP$^+$ cells (22.2% ± 5.0%, $P < 0.02$; Supplementary Fig. S1A). ICC showed that increasing concentrations of Activin A induced increasing numbers of Foxa2$^+$ cells and that a high number of T-GFP$^+$Foxa2$^+$ double-positive cells formed only when the cells were differentiated in 1 ng/mL Activin A (Supplementary Fig. S1B). We next determined if Foxa2$^+$T$^+$ cells could be differentiated further toward a Noto-expressing node/notochord-like cell fate by manipulating Wnt, BMP, and RA signaling. After incubation of *Noto*$^{Gfp/+}$ cells with 1 ng/mL Activin A for 3 days the medium was supplemented with relevant growth factors or their inhibitors for another 2 days (Fig. 2A). While treatment with Wnt3a did not change the number of Noto-GFP$^+$ cells, we found that inhibition of canonical Wnt signaling using Dkk1 tended to increase the percentage of Noto-GFP$^+$ cells, but the effect was marginal and did not reach statistical significance (Fig. 2A). Addition of BMP4 or RA reduced the number of Noto-GFP$^+$ cells from 1.5% ± 0.5% to 0.9% ± 0.2% not significant (n.s.) and 0.4% ± 0.2% ($P < 0.03$), respectively (Fig. 2A). This effect could be reversed by addition of Noggin or the RA inhibitor AGN193109, respectively. Notably, inhibition of endogenous BMP or RA signaling, by addition of Noggin or AGN193109, increased the number of Noto-GFP$^+$ cells to 2.7 ± 0.6% (n.s.) and 3.7% ± 1.1% ($P < 0.05$), respectively (Fig. 2A).

Based on the ability of RA and BMP antagonists to augment differentiation of Noto-GFP$^+$ cells and on Xenopus data showing that co-repression of BMP and Wnt signaling is essential for *Xnot* induction [22], we next tested if the simultaneous inhibition of these signaling pathways could stimulate development of Noto-GFP$^+$ cells. We performed these experiments in the absence or presence of 100 ng/mL Fgf2 to test if Fgf signaling would influence the differentiation of Noto-GFP$^+$ cells. Different combinations of Noggin, Dkk1, and AGN193109 showed that a combination of AGN193109 and either Noggin or Dkk1

resulted in induction of Noto-GFP$^+$ cells as did the simultaneous inhibition of all 3 pathways (Fig. 2B). Additional treatment with Fgf2 was found to enhance the development of Noto-GFP$^+$ cells (Fig. 2B). However, in some experiments the combination of AGN193109 and Noggin gave better induction than AGN193109 and Dkk1, but in other experiments the opposite result was seen, likely due to variability in endogenous signaling. Further experiments were therefore performed in the presence of Activin A and Fgf2 and with simultaneous inhibition of the BMP, Wnt and RA pathways (Fig. 2C).

Studies in several species suggest that inhibition of Notch signaling drives differentiation of midline precursor cells into notochord at the expense of floor plate/hypochord formation [24-29]. Addition of the γ-secretase inhibitor Compound XVIII, which inhibits the proteolytic cleavage of the Notch receptor, tended to increase the number of Noto-GFP$^+$ cells when differentiated with the 2 step protocol, but the effect did not reach statistical significance (Supplementary Fig. S2A).

During early development different types of Fgfs are expressed and knockout studies have demonstrated their important role in mesoderm formation and gastrulation movements (reviewed by ref. [39]). Therefore, we tested whether the application of Fgf4 or Fgf8 instead of Fgf2 could increase the induction of Noto-GFP expression. Fgf4 yielded results comparable to Fgf2, whereas Fgf8 had no positive effect on Noto-GFP induction (Supplementary Fig. S2B).

Since the zebrafish Noto homolog *flh* appears to positively regulate its own expression [40], we investigated whether transfection of *Noto*$^{Gfp/+}$ cells with an expression vector encoding Noto-IRES-dTomato could influence development of Noto-GFP$^+$ cells. FACS analysis of the GFP signal in dTomato$^+$ cells showed a significant increase in Noto-GFP$^+$ cells in the presence of 1 ng/mL Activin A from 5.2% ± 1% to 10.7% ± 2.8% ($P < 0.05$; Fig. 2D), indicating that Noto can induce its own expression even in the absence of the inhibitors that were applied during the second step of the differentiation protocol. Still, the earliest that a GFP signal could be detected was at day 4 to 5 of differentiation, demonstrating that the expression of Noto itself cannot accelerate differentiation and that the differentiation process might have to pass through the Foxa2$^+$T$^+$ precursor state.

Characterization of in vitro derived Noto-GFP$^+$ cells

To characterize the Noto-GFP$^+$ cells, we FACS sorted GFP$^+$ and GFP$^-$ populations after 5 days of differentiation with the 2-step protocol. FACS sorting at day 5 enriched the Noto-GFP$^+$ population from 10% to above 90% purity. QRT-PCR analysis showed a 25-fold upregulation of *Noto* mRNA in Noto-GFP$^+$ cells compared with GFP$^-$ cells (Fig. 3A). The node and notochord markers *Foxa2* and *T* were also enriched in the GFP$^+$ population. ICC for GFP (Noto), Foxa2, and T confirmed the co-expression of Noto and Foxa2 as well as Noto and T in day 5 cultures (Fig. 3B). The notochord secretes Shh to pattern adjacent tissues, including the neural tube and the myotome [6,8,41]. mRNA levels of *Shh* were strongly enriched in Noto-GFP$^+$ cells (Fig. 3A) and Shh protein could be detected in Noto-GFP$^+$ cells by ICC (Fig. 3B, lowest panel). Since a grafted notochord can induce ectopic floor plate development in chicken neural tube [7] and since Shh is the mediator of neural tube patterning [42,43], we tested if grafting of Noto-GFP$^+$ cells could induce an ectopic floor plate. When Noto-GFP$^+$ cells were grafted lateral to the neural tube into HH st 8–10 chicken embryos [44], whole-mount immunostaining revealed an expansion of the floor plate marker Foxa2 toward the side where the graft is placed (2/21 embryos; Fig. 3C).

The node and the notochord also produce the BMP antagonists Chordin and Noggin. Both markers showed a high mRNA expression level in Noto-GFP$^+$ cells (Fig. 3A). *Nodal* was also expressed, but not enriched, in the Noto-GFP$^+$ cell population and could be detected

during the entire differentiation process (Fig. 3A). In contrast, expression of the node marker *Foxj1* was highly enriched in the Noto-GFP$^+$ cell fraction (Fig. 3A). As the node can give rise to both notochord and floor plate, we further tested whether the floor plate marker *Arx* was expressed in our cell culture system. Indeed, *Arx* expression was enriched in the Noto-GFP$^+$ cell fraction at day 5 (Fig. 3A), indicating that some Noto-GFP$^+$ cells might be able to further give rise to floor plate. *Gsc*, *Lim1*, *Otx2*, and Cerberus-like 1 (*Cer1*) are important regulators in the gastrulating embryo and are, besides other tissues, expressed in the anterior most part of the PS that will give rise to the node. All 4 genes are induced during the 2-step differentiation protocol but show no specific enrichment within the Noto-GFP$^+$ cell population (Supplementary Fig. S3).

During development the notochord has, besides patterning the surrounding tissues, also an essential function as structural support for the embryo. Its extracellular matrix and the vacuolarized cells make the notochord a rigid organ that functions as skeletal element in lower vertebrate embryos important for embryo elongation and locomotion. In mouse embryos, the notochord cells present an abundant presence of cytoplasmic vacuoles around embryonic day 14 caused by excessive dilation of the endoplasmic reticulum and mitochondria [45]. Transmission electron microscopy analysis of in vitro derived Noto-GFP$^+$ cells showed enlarged, dilated mitochondria comparable to those described in mouse embryos (Fig. 3D) [45]. Together, these data demonstrate that in vitro derived Noto-GFP$^+$ cells express node, notochord, and floor plate markers and that some Noto-GFP$^+$ cells exhibit a vacuolarization typical of the notochord. The presence of these markers indicates that the ES cell-derived Noto-GFP$^+$ cells may represent a heterogeneous mix of node-like cells and their immediate progeny: notochord and floor plate cells. Evidently, a large population of Noto-GFP$^-$ cells is present in our cultures. In order to determine the identity of these cells, we analyzed for the mesodermal markers *Mesp1* and *Flk1* as well as the endodermal markers *Sox17* and *Cer1*. Expression of all markers could be detected in the GFP$^-$ fraction of the day 5 cultures as well as in the vehicle-treated controls (Supplementary Fig. S3A). Triple ICC demonstrated that many of the GFP$^-$ cells were either Flk1$^+$ or Sox17$^+$ (Supplementary Fig. S3B), indicating that significant amounts of non-axial mesoderm as well as some endoderm are formed in our cultures.

Proliferation and maintenance of Noto-GFP$^+$ cells

A closer inspection of the Noto-GFP expression over time showed that the percentage of Noto-GFP$^+$ cells was maintained over time, whereas the absolute number of Noto-GFP$^+$ cells increased (Fig. 4A, B). This observation raised the question whether the increasing pool of Noto-GFP$^+$ cells came from newly differentiated Noto-GFP$^+$ cells or through proliferation of the existing Noto-GFP$^+$ pool. Initially, Fgfs were discovered as having mitogenic effect on fibroblast cells and could therefore be candidates of inducing a mitogenic response in Noto-GFP$^+$ cells [46,47]. Hence, we determined the number of proliferating Noto-GFP$^+$ cells in the presence or absence of Fgf2 by EdU incorporation. No significant difference between the proliferation rates with or without Fgf2 could be detected (Fig. 4C, D). Still, there is a tendency that in the presence of Fgf2 more of the Noto-GFP$^+$ cells incorporated EdU. Overall, these data indicate that most of the Noto-GFP$^+$ cells are derived from newly differentiated cells but that the existing pool of Noto-GFP$^+$ cells also had the ability to proliferate.

Studies in mouse have shown that both Shh and canonical Wnt signaling are important in the maintenance, but not the formation, of the notochord. Knockout of Shh as well as notochord-specific ablation of beta-catenin initially lead to a reduction of *T* expression in the posterior end of the notochord and eventually resulted in a loss of *T* expression and subsequently of the notochord in the tail after e9.5 and e10.5, respectively [48,49].

Therefore, we investigated whether Shh and Wnt3a as well as Fgf2 could augment proliferation and maintenance of the differentiated Noto-GFP$^+$ pool by culturing them in a third step for up to 3 days in the presence of a single growth factor or in combinations of them (Fig. 5A). As a control we continued culture in step 2 medium. FACS analysis demonstrated that the percentage of Noto-GFP$^+$ cells dropped over time in all conditions (Fig. 5B). The presence of Fgf2 had a positive effect on the Noto-GFP expression but the continuation with the step 2 medium resulted in the highest percentage of Noto-GFP$^+$ cells up to day 8. All conditions increased the total cell number over time with a combination of Fgf2 and Wnt3a, yielding the highest total cell numbers (Fig. 5C). Based on percentage Noto-GFP$^+$ and total cell number per well the absolute cell number of Noto-GFP$^+$ cells per well was calculated. When the growth factors had been applied alone the absolute cell number dropped from day 6 on. In the presence of combinations of 2 of the growth factors the absolute number of Noto-GFP$^+$ cells peaked at day 6 and started to decline only from day 7. If Fgf2, Wnt3a, and Shh were combined together, the absolute number of Noto-GFP$^+$ cells increased until day 7 and started to decline slowly at day 8. Similar results were seen in the presence of the step 2 medium (Fig. 5D). These results suggest that both Wnt3a and Shh together with Fgf2 have the potential to increase and maintain the Noto-GFP$^+$ cell population for a limited time in vitro. An obvious experiment would be the application of these growth factors to a pure Noto-GFP$^+$ population instead of a heterogenous cell culture with its undefined endogenous signaling, but unfortunately, all attempts to isolate Noto-GFP$^+$ cells failed as the cells did not survive FACS-based cell sorting and re-plating.

ES cell-derived Noto-GFP$^+$ cells can contribute to midline structures when grafted to chicken embryos

Previous work has demonstrated that when the medial sector of Hensen's node from a quail or GFP-expressing chicken is grafted into the same region of the node of a host chicken embryo, it can contribute to midline structures such as floor plate and notochord in the host embryo [5,29]. To test the ability of our in vitro derived node/notochord-like cells to contribute to derivatives of the node, we grafted Noto-GFP$^+$ cells into the node of explanted HH st 4 chicken embryos. Many of the embryos had a truncated body most likely due to the removal of node cells and the limited ability of the mouse ES cells to proliferate and contribute to the chicken embryo. Nevertheless, a few embryos showed a partial contribution of the grafted ESC-derived cells to the midline structures of the host embryos (Fig. 6A). After grafting Noto-GFP$^+$ cells at HH st 4, we could detect ES cell progeny in the notochord (3/13 embryos; Fig. 6B), indicating that the grafted Noto-GFP$^+$ cells can contribute to the notochord in the host embryo. Some grafted cells, including GFP$^+$ and GFP$^-$ cells, were further found in the endoderm (Fig. 6C), which has been observed previously and been shown to be caused by the grafting procedure [5]. The GFP$^-$ cells might represent the rare endodermal cells that also formed in our culture and even with manual picking of GFP-positive cell clusters, a contamination with GFP-negative cells could not be excluded.

Discussion

Here we have isolated and charaterized a node/notochord-like cell population derived from mouse ES cells using a *Noto*$^{Gfp/+}$ reporter cell line. Consistent with knockout studies in the mouse [12] in vitro differentiation toward an axial midline fate was stimulated when a Foxa2$^+$T$^+$ precursor population was first induced by a low concentration of Activin A. In a second step, continued low Activin A together with Fgf2 and the inhibitors AGN193109, Dkk1, and Noggin was able to boost the numbers of Noto-GFP-expressing cells that co-expressed Foxa2 and T. Studies in Xenopus showed that a co-repression of BMP and Wnt signaling is required for notochord development [22]. Strikingly, in our in vitro mouse

system we could further show that RA at physiologically levels inhibits node/notochord differentiation and that inhibition of endogenous RA signaling had a beneficial effect on the formation of Noto-GFP$^+$ cells. This appears to conflict with data from the chicken embryo, where RA has been shown to act as inducer of *Gnot1* expression [23]. However, even though *Raldh2* is expressed in E6.75 node cells and the RARE-LacZ reporter suggests active RA signaling at this stage in node cells, the functional significance of this signaling is uncertain. It may act inhibitory to notochord formation as *Raldh2* mutants have an enlarged notochord [50]. Also, high concentrations of Activin A or Nodal inhibited Noto induction and this result correlates well with studies from other species where low Nodal concentrations induce *flh*, whereas high concentration favors *gsc* induction [18,19,51]. Increasing concentrations of Activin A induced increasing numbers of Foxa2$^+$ cells, whereas T expression was strongly inhibited by high Activin A and had its maximum at the low Activin A concentration of 1 ng/mL. At the same concentration the most cells co-expressing Foxa2 and T were detected. Thus, high levels of Activin A lowered the number of Noto-GFP$^+$ cells by inhibiting T induction and driving the Foxa2$^+$ cells toward a definitive endoderm fate as this has been shown in different ES cell differentiation studies [35,52] and where Foxa2 is known to be expressed [53,54].

The ability of transfected *Noto* cDNA to induce endogenous *Noto* expression is consistent with data from zebrafish that showed loss of *flh* mRNA in *flh* mutants [40]. However, in the mouse loss of Noto function results in persistent *Noto* expression, suggesting that it is required for its own repression [12]. It has been suggested that an unknown factor is responsible for the anterior notochord development seen in mouse *Noto* mutants [12] and it is possible that this putative factor could also be responsible for the apparently normal Noto expression (as assayed by GFP expression) in *Noto*$^{Gfp/Gfp}$ embryos. Thus, our gain-of-function data may reveal a positive role for mouse Noto in its own expression that is not readily apparent from loss-of-function studies.

Noto expression is exclusively detectable in node and notochord tissue [12]. Marker analysis as well as morphology indicated that cells similar to both tissues were present within our Noto-GFP$^+$ population. This is further supported by the grafting experiments where progeny of grafted Noto-GFP$^+$ cells can be found in the notochord. Moreover, expression of the floor plate marker *Arx* suggested that a node-like subpopulation might not only be able to further differentiate into notochord but also to give rise to floor plate-like cells. Alternatively, we may derive a homogenous population of progenitors that express markers of the node as well as its progeny. This question cannot be resolved from our qPCR data and would require the identification of cell surface markers that potentially could be used to isolate distinct subpopulations within the Noto-GFP$^+$ population.

Together with Foxa2 and T, the homeobox genes *Gsc, Lim1*, and *Otx2* are co-expressed in the early gastrula organizer of the mouse at the anterior end of the PS were the node will form (reviewed by ref. [55]). Lim1 has further been shown to co-localize with Foxa2 in the node [56]. Also, Cer1 is a marker of the anterior half of the mouse embryo. Even though Cer1 expression is excluded from the node its mRNA can be detected in the anterior mesendoderm as well as the prechordal and the notochordal plate [57]. As expected their expression was not particularly upregulated in the Noto-GFP$^+$ cells but indicated that an environment similar to that in the anterior embryo was created, which is required for the node formation and further notochord development. The application of extrinsic factors might be required for the node/notochord formation as well as cell-cell contacts with supporting mesodermal and endodermal tissues. We cannot exclude that some of the non-axial cell populations formed in our cultures express inhibitory factors that prevents further differentiation or proliferation of Noto-GFP$^+$ cells. Such inhibitory signals might also limit proliferation and maintenance of Noto-GFP$^+$ cells within this heterogeneous cell mixture.

The node and the notochord secrete growth factors and signaling molecules with inductive activities. Most intensely studied is Shh and the dorso-ventral patterning of the neural tube [6,41] and the BMP antagonists Chordin and Noggin, which are important in forebrain development [58], vessel formation [59,60], and left-right axis establishment [61]. The presence of these factors within the Noto-GFP$^+$ cell population suggests that in vitro derived node/notochord-like cells could pattern adjacent cells in a culture dish. A node/notochord-like cell population as described here represents an interesting tool: not only for its potential ability to induce patterning in other ES cell-derived populations, but also for the biochemical characterization of axial midline cells that will benefit from the unlimited availability of in vitro derived cells.

Supplementary Material

Refer to Web version on PubMed Central for supplementary material.

Acknowledgments

We thank Achim Gossler for providing the Noto-GFP ES cells, and Søren R. Lindskog and Hanne M. Mølbak Holm for excellent technical assistance. We also thank Shona Gray for sharing her expertise in grafting of the Hensen's node in chicken embryos. This work was supported by DASCDOC, the EU 6th Framework Program, and the JDRF.

References

1. Spemann H, Mangold H. Über Induktion von Embryonalanlagen durch Implantation artfremder Organisatoren. Roux Arch EntwMech Org. 1924:599–638.
2. Nonaka S, Shiratori H, Saijoh Y, Hamada H. Determination of left-right patterning of the mouse embryo by artificial nodal flow. Nature. 2002; 418:96–99. [PubMed: 12097914]
3. Nonaka S, Tanaka Y, Okada Y, Takeda S, Harada A, Kanai Y, Kido M, Hirokawa N. Randomization of left-right asymmetry due to loss of nodal cilia generating leftward flow of extraembryonic fluid in mice lacking KIF3B motor protein. Cell. 1998; 95:829–837. [PubMed: 9865700]
4. Okada Y, Nonaka S, Tanaka Y, Saijoh Y, Hamada H, Hirokawa N. Abnormal nodal flow precedes situs inversus in iv and inv mice. Mol Cell. 1999; 4:459–468. [PubMed: 10549278]
5. Le Douarin NM, Halpern ME. Discussion point. Origin and specification of the neural tube floor plate: insights from the chick and zebrafish. Curr Opin Neurobiol. 2000; 10:23–30. [PubMed: 10679443]
6. Yamada T, Placzek M, Tanaka H, Dodd J, Jessell TM. Control of cell pattern in the developing nervous system: polarizing activity of the floor plate and notochord. Cell. 1991; 64:635–647. [PubMed: 1991324]
7. Placzek M, Tessier-Lavigne M, Yamada T, Jessell T, Dodd J. Mesodermal control of neural cell identity: floor plate induction by the notochord. Science. 1990; 250:985–988. [PubMed: 2237443]
8. Currie PD, Ingham PW. Induction of a specific muscle cell type by a hedgehog-like protein in zebrafish. Nature. 1996; 382:452–455. [PubMed: 8684485]
9. Kim SK, Hebrok M, Melton DA. Notochord to endoderm signaling is required for pancreas development. Development. 1997; 124:4243–4252. [PubMed: 9334273]
10. Hebrok M, Kim SK, Melton DA. Notochord repression of endodermal Sonic hedgehog permits pancreas development. Genes Dev. 1998; 12:1705–1713. [PubMed: 9620856]
11. Yamamoto M, Meno C, Sakai Y, Shiratori H, Mochida K, Ikawa Y, Saijoh Y, Hamada H. The transcription factor FoxH1 (FAST) mediates Nodal signaling during anterior-posterior patterning and node formation in the mouse. Genes Dev. 2001; 15:1242–1256. [PubMed: 11358868]
12. Abdelkhalek HB, Beckers A, Schuster-Gossler K, Pavlova MN, Burkhardt H, Lickert H, Rossant J, Reinhardt R, Schalkwyk LC, Muller I, Herrmann BG, Ceolin M, Rivera-Pomar R, Gossler A. The

mouse homeobox gene Not is required for caudal notochord development and affected by the truncate mutation. Genes Dev. 2004; 18:1725–1736. [PubMed: 15231714]

13. Ang SL, Rossant J. HNF-3 beta is essential for node and notochord formation in mouse development. Cell. 1994; 78:561–574. [PubMed: 8069909]
14. Weinstein DC, Ruiz A, Altaba i, Chen WS, Hoodless P, Prezioso VR, Jessell TM, Darnell JE Jr. The winged-helix transcription factor HNF-3 beta is required for notochord development in the mouse embryo. Cell. 1994; 78:575–588. [PubMed: 8069910]
15. Herrmann BG, Labeit S, Poustka A, King TR, Lehrach H. Cloning of the T gene required in mesoderm formation in the mouse. Nature. 1990; 343:617–622. [PubMed: 2154694]
16. Yamanaka Y, Tamplin OJ, Beckers A, Gossler A, Rossant J. Live imaging and genetic analysis of mouse notochord formation reveals regional morphogenetic mechanisms. Dev Cell. 2007; 13:884–896. [PubMed: 18061569]
17. Herrmann BG. Expression pattern of the Brachyury gene in whole-mount TWis/TWis mutant embryos. Development. 1991; 113:913–917. [PubMed: 1821859]
18. Gritsman K, Talbot WS, Schier AF. Nodal signaling patterns the organizer. Development. 2000; 127:921–932. [PubMed: 10662632]
19. Chen Y, Schier AF. The zebrafish Nodal signal Squint functions as a morphogen. Nature. 2001; 411:607–610. [PubMed: 11385578]
20. von Dassow G, Schmidt JE, Kimelman D. Induction of the Xenopus organizer: expression and regulation of Xnot, a novel FGF and activin-regulated homeo box gene. Genes Dev. 1993; 7:355–366. [PubMed: 8095482]
21. Lustig KD, Kroll K, Sun E, Ramos R, Elmendorf H, Kirschner MW. A Xenopus nodal-related gene that acts in synergy with noggin to induce complete secondary axis and notochord formation. Development. 1996; 122:3275–3282. [PubMed: 8898239]
22. Yasuo H, Lemaire P. Role of Goosecoid, Xnot and Wnt antagonists in the maintenance of the notochord genetic programme in Xenopus gastrulae. Development. 2001; 128:3783–3793. [PubMed: 11585804]
23. Knezevic V, Ranson M, Mackem S. The organizer-associated chick homeobox gene, Gnot1, is expressed before gastrulation and regulated synergistically by activin and retinoic acid. Dev Biol. 1995; 171:458–470. [PubMed: 7556928]
24. Appel B, Fritz A, Westerfield M, Grunwald DJ, Eisen JS, Riley BB. Delta-mediated specification of midline cell fates in zebrafish embryos. Curr Biol. 1999; 9:247–256. [PubMed: 10074451]
25. Latimer AJ, Dong X, Markov Y, Appel B. Delta-Notch signaling induces hypochord development in zebrafish. Development. 2002; 129:2555–2563. [PubMed: 12015285]
26. Latimer AJ, Appel B. Notch signaling regulates midline cell specification and proliferation in zebrafish. Dev Biol. 2006; 298:392–402. [PubMed: 16876779]
27. Lopez SL, Paganelli AR, Siri MV, Ocana OH, Franco PG, Carrasco AE. Notch activates sonic hedgehog and both are involved in the specification of dorsal midline cellfates in Xenopus. Development. 2003; 130:2225–2238. [PubMed: 12668635]
28. Lopez SL, Rosato-Siri MV, Franco PG, Paganelli AR, Carrasco AE. The Notch-target gene hairy2a impedes the involution of notochordal cells by promoting floor plate fates in Xenopus embryos. Development. 2005; 132:1035–1046. [PubMed: 15689375]
29. Gray SD, Dale JK. Notch signalling regulates the contribution of progenitor cells from the chick Hensen's node to the floor plate and notochord. Development. 2010; 137:561–568. [PubMed: 20110321]
30. Fehling HJ, G Lacaud, Kubo A, Kennedy M, Robertson S, Keller G, Kouskoff V. Tracking mesoderm induction and its specification to the hemangioblast during embryonic stem cell differentiation. Development. 2003; 130:4217–4227. [PubMed: 12874139]
31. Ying QL, Nichols J, Chambers I, Smith A. BMP induction of Id proteins suppresses differentiation and sustains embryonic stem cell self-renewal in collaboration with STAT3. Cell. 2003; 115:281–292. [PubMed: 14636556]
32. Silva J, Barrandon O, Nichols J, Kawaguchi J, Theunissen TW, Smith A. Promotion of reprogramming to ground state pluripotency by signal inhibition. PLoS Biol. 2008; 6:e253. [PubMed: 18942890]

33. Inman GJ, Nicolás FJ, Callahan JF, Harling JD, Gaster LM, Reith AD, Laping NJ, Hill CS. SB-431542 is a potent and specific inhibitor of transforming growth factor-beta superfamily type I activin receptor-like kinase (ALK) receptors ALK4, ALK5 and ALK7. Mol Pharmacol. 2002; 62:65–74. [PubMed: 12065756]
34. Kochhar DM, Jiang H, Penner JD, Johnson AT, Chandraratna RA. The use of a retinoid receptor antagonist in a new model to study vitamin A-dependent developmental events. Int J Dev Biol. 1998; 42:601–608. [PubMed: 9694631]
35. Hansson M, Olesen DR, Peterslund JM, Engberg N, Kahn M, Winzi M, Klein T, Maddox-Hyttel P, Serup P. A late requirement for Wnt and FGF signaling during activin-induced formation of foregut endoderm from mouse embryonic stem cells. Dev Biol. 2009; 330:286–304. [PubMed: 19358838]
36. Hyttel P, Madsen I. Rapid method to prepare mammalian oocytes and embryos for transmission electron microscopy. Acta Anat (Basel). 1987; 129:12–14. [PubMed: 3618092]
37. Chapman SC, Collignon J, Schoenwolf GC, Lumsden A. Improved method for chick whole-embryo culture using a filter paper carrier. Dev Dyn. 2001; 220:284–289. [PubMed: 11241836]
38. Ahnfelt-Ronne J, Jorgensen MC, Hald J, Madsen OD, Serup P, Hecksher-Sorensen J. An improved method for three-dimensional reconstruction of protein expression patterns in intact mouse and chicken embryos and organs. J Histochem Cytochem. 2007; 55:925–930. [PubMed: 17478445]
39. Bottcher RT, Niehrs C. Fibroblast growth factor signaling during early vertebrate development. Endocr Rev. 2005; 26:63–77. [PubMed: 15689573]
40. Melby AE, Kimelman D, Kimmel CB. Spatial regulation of floating head expression in the developing notochord. Dev Dyn. 1997; 209:156–165. [PubMed: 9186051]
41. Placzek M, Yamada T, Tessier-Lavigne M, Jessell T, Dodd J. Control of dorsoventral pattern in vertebrate neural development: induction and polarizing properties of the floor plate. Development. 1991; (Suppl 2):105–122. [PubMed: 1842349]
42. Ericson J, Morton S, Kawakami A, Roelink H, Jessell TM. Two critical periods of Sonic Hedgehog signaling required for the specification of motor neuron identity. Cell. 1996; 87:661–673. [PubMed: 8929535]
43. Tanabe Y, Jessell TM. Diversity and pattern in the developing spinal cord. Science. 1996; 274:1115–1123. [PubMed: 8895454]
44. Hamburger V, Hamilton HL. A series of normal stages in the development of the chick embryo. 1951. Dev Dyn. 1992; 195:231–272. [PubMed: 1304821]
45. Jurand A. Some aspects of the development of the notochord in mouse embryos. J Embryol Exp Morphol. 1974; 32:1–33. [PubMed: 4141719]
46. Armelin HA. Pituitary extracts and steroid hormones in the control of 3T3 cell growth. Proc Natl Acad Sci U S A. 1973; 70:2702–2706. [PubMed: 4354860]
47. Gospodarowicz D. Localisation of a fibroblast growth factor and its effect alone and with hydrocortisone on 3T3 cell growth. Nature. 1974; 249:123–127. [PubMed: 4364816]
48. Chiang C, Litingtung Y, Lee E, Young KE, Corden JL, Westphal H, Beachy PA. Cyclopia and defective axial patterning in mice lacking Sonic hedgehog gene function. Nature. 1996; 383:407–413. [PubMed: 8837770]
49. Ukita K, Hirahara S, Oshima N, Imuta Y, Yoshimoto A, Jang CW, Oginuma M, Saga Y, Behringer RR, Kondoh H, Sasaki H. Wnt signaling maintains the notochord fate for progenitor cells and supports the posterior extension of the notochord. Mech Dev. 2009; 126:791–803. [PubMed: 19720144]
50. Ribes V, Le Roux I, Rhinn M, Schuhbaur B, Dolle P. Early mouse caudal development relies on crosstalk between retinoic acid, Shh and Fgf signalling pathways. Development. 2009; 136:665–676. [PubMed: 19168680]
51. Green JB, New HV, Smith JC. Responses of embryonic Xenopus cells to activin and FGF are separated by multiple dose thresholds and correspond to distinct axes of the mesoderm. Cell. 1992; 71:731–739. [PubMed: 1423628]
52. Kubo A, Shinozaki K, Shannon JM, Kouskoff V, Kennedy M, Woo S, Fehling HJ, Keller G. Development of definitive endoderm from embryonic stem cells in culture. Development. 2004; 131:1651–1662. [PubMed: 14998924]

53. Ang SL, Wierda A, Wong D, Stevens KA, Cascio S, Rossant J, Zaret KS. The formation and maintenance of the definitive endoderm lineage in the mouse: involvement of HNF3/forkhead proteins. Development. 1993; 119:1301–1315. [PubMed: 8306889]

54. Monaghan AP, Kaestner KH, Grau E, Schutz G. Postimplantation expression patterns indicate a role for the mouse forkhead/HNF-3 alpha, beta and gamma genes in determination of the definitive endoderm, chordamesoderm and neuroectoderm. Development. 1993; 119:567–578. [PubMed: 8187630]

55. Camus A, Tam PP. The organizer of the gastrulating mouse embryo. Curr Top Dev Biol. 1999; 45:117–153. [PubMed: 10332604]

56. Perea-Gomez A, Shawlot W, Sasaki H, Behringer RR, Ang S. HNF3beta and Lim1 interact in the visceral endoderm to regulate primitive streak formation and anterior-posterior polarity in the mouse embryo. Development. 1999; 126:4499–4511. [PubMed: 10498685]

57. Biben C, Stanley E, Fabri L, Kotecha S, Rhinn M, Drinkwater C, Lah M, Wang CC, Nash A, Hilton D, Ang SL, Mohun T, Harvey RP. Murine cerberus homologue mCer-1: a candidate anterior patterning molecule. Dev Biol. 1998; 194:135–151. [PubMed: 9501024]

58. Bachiller D, Klingensmith J, Kemp C, Belo JA, Anderson RM, May SR, McMahon JA, McMahon AP, Harland RM, Rossant J, De Robertis EM. The organizer factors Chordin and Noggin are required for mouse forebrain development. Nature. 2000; 403:658–661. [PubMed: 10688202]

59. Reese DE, Hall CE, Mikawa T. Negative regulation of midline vascular development by the notochord. Dev Cell. 2004; 6:699–708. [PubMed: 15130494]

60. Bressan M, Davis P, Timmer J, Herzlinger D, Mikawa T. Notochord-derived BMP antagonists inhibit endothelial cell generation and network formation. Dev Biol. 2009; 326:101–111. [PubMed: 19041859]

61. Mine N, Anderson RM, Klingensmith J. BMP antagonism is required in both the node and lateral plate mesoderm for mammalian left-right axis establishment. Development. 2008; 135:2425–2434. [PubMed: 18550712]

Europe PMC Funders Author Manuscripts

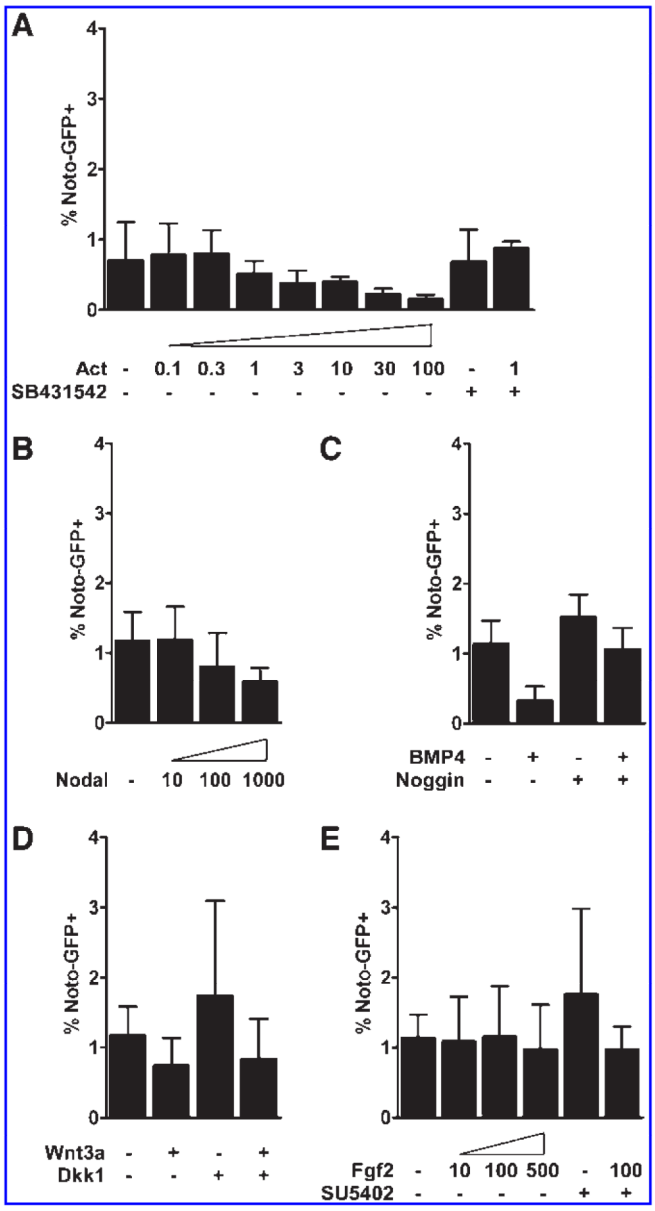

FIG. 1.

Inhibition of Noto-GFP expression by high Activin A concentration and BMP4. FACS analysis of Noto-GFP expression after 4 days of culture in the presence of (**A**) 0.1–100 ng/mL Activin A and 10 μM SB431542, (**B**) 10-1000 ng/mL Nodal, (**C**) 10 ng/mL BMP4 and 50 ng/mL Noggin, (**D**) 50 ng/mL Wnt3a and 320 ng/mL Dkk1, and (**E**) 10-500 ng/mL Fgf2 and 1 μM SU5402. The data represent the mean ± SD of at least 3 independent experiments. See also Supplementary Fig. S1. FACS, fluorescence-activated cell sorting; SD, standard deviation.

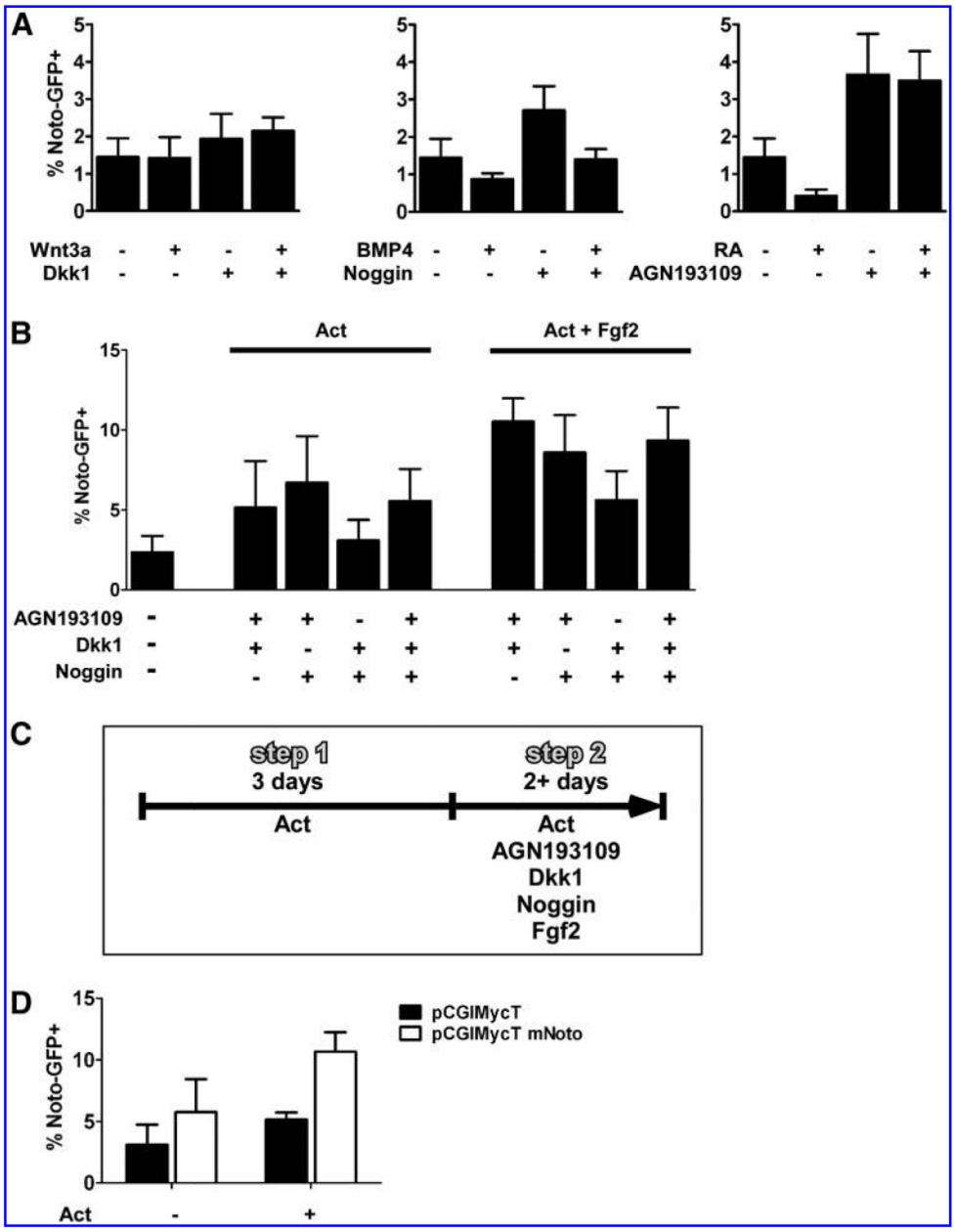

FIG. 2.

Noto induction requires simultaneous inhibition of BMP, Wnt, and RA signaling. FACS analysis of Noto-GFP expression after 5 days of culture in the presence of different growth factors. The data represent the mean ± SD of at least 3 experiments. (**A**) Cells were cultured for 3 days in the presence of 1 ng/mL Activin A. During days 4 and 5 the medium was additionally to Activin A supplemented with growth factors and/or their inhibitors: 50 ng/mL Wnt3a, 320 ng/mL Dkk1, 10 ng/mL BMP4, 50 ng/mL Noggin, 0.1 μM RA, and 10 μM AGN193109. (**B**) Cells were cultured for 3 days in the presence of 1 ng/mL Activin A. During day 4 and 5 the medium was in addition to 1 ng/mL Activin A or 1 ng/mL Activin A plus 100 ng/mL Fgf2, supplemented with 10 μM AGN193109, 320 ng/mL Dkk1, and 50 ng/mL Noggin and the different combinations of them. (**C**) Schematic view of the final differentiation protocol. (**D**) FACS analysis of Noto-GFP expression after 5 days of

differentiation with or without 1 ng/mL Activin A. After 1 day of differentiation cells were transfected with a Noto-IRES-dTomato plasmid. Ninety-six hours after transfection FACS analysis was performed. Therefore, GFP expression within the dTomato^{+} cell population was measured. See also Supplementary Fig. S2. RA, retinoic acid.

Europe PMC Funders Author Manuscripts

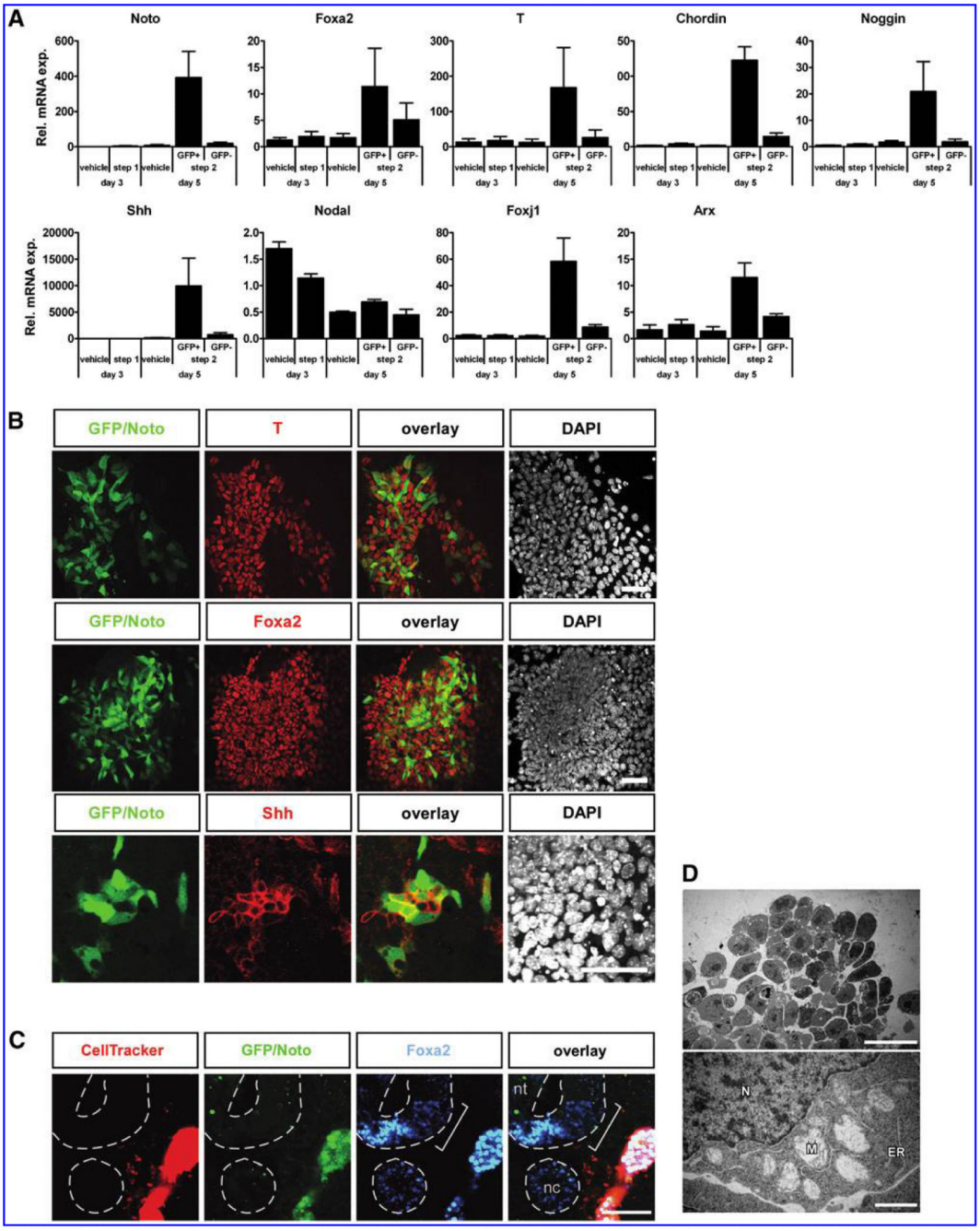

FIG. 3.

Characterization of Noto-GFP $^{+}$ cells. (**A**) Quantitative reverse transcriptase-polymerase chain reaction analysis of marker expression during differentiation of Noto$^{Gfp/+}$ ES cells. The ratio of gene expression against undifferentiated Noto$^{Gfp/+}$ ES cells is shown. The data represents the mean ± standard error of the mean of at least 3 independent experiments. (**B**) Immunocytochemistry of T, Foxa2, Shh (*red*), and GFP (*green*) in Noto$^{Gfp/+}$ cells was performed at day 5 of the differentiation process. Cell nuclei were stained with DAPI (*white*). Scale bar = 50 μm. (**C**) Transverse section of a chicken embryo with the Noto-GFP $^{+}$ graft lateral to the neural tube. The *bracket* indicates the expanded Foxa2^{+} region

Europe PMC Funders Author Manuscripts

toward the graft. nt, neural tube; nc, notochord; Scale bar = 50 μm. (**D**) Transmission electron micrograph of Noto-GFP $^{+}$ cell clusters. Note the dilated mitochondria (M) adjacent to the nucleus (N) and undilated rough endoplasmic reticulum (ER). Scale bars = 20 μm (*upper*) and 1 μm (*lower*). See also Supplementary Fig. S3. ES, embryonic stem.

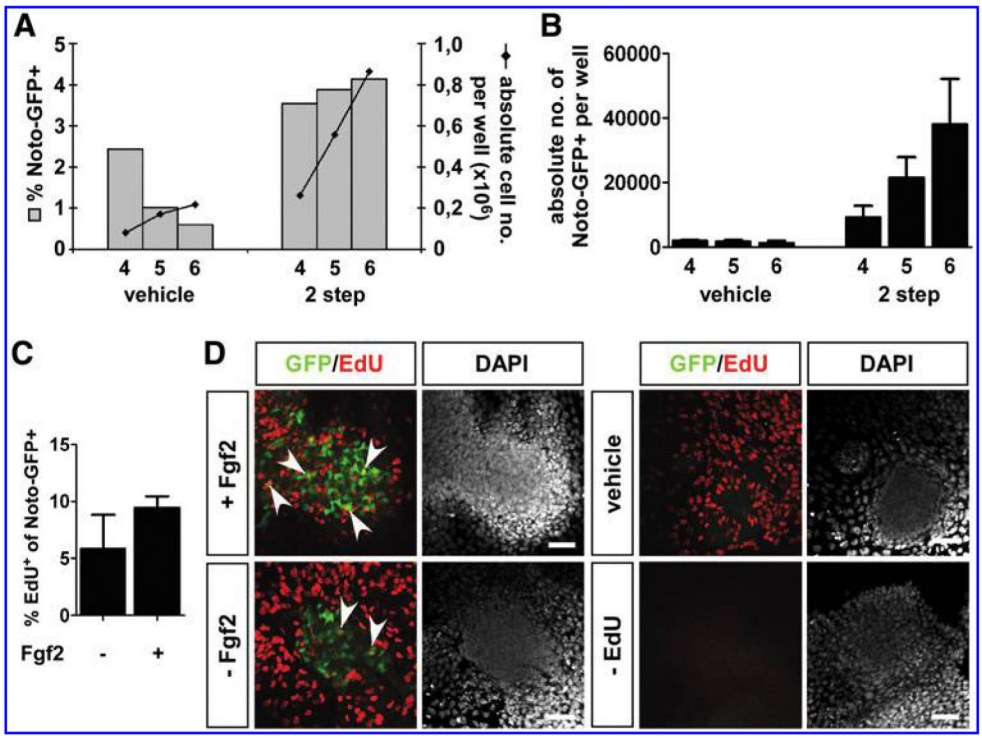

FIG. 4.

Proliferation of Noto-GFP$^+$ cells. (**A**) FACS analysis of differentiating Noto-GFP ES cells at day 4 to 6. At the same time points the absolute cell number for each well was counted. (**B**) Based on % Noto-GFP$^+$ and total cell number per well the absolute cell number of Noto-GFP$^+$ cells per well was determined. (**C**) The proliferation of Noto-GFP$^+$ cells in the presence or absence of Fgf2 was analyzed by EdU incorporation. Data represents the % EdU$^+$GFP$^+$ cells within the Noto-GFP$^+$ cell population of 3 independent experiments (mean ± standard error of the mean). (**D**) Immunocytochemistry of EdU (*red*) and GFP (*green*). Cell nuclei were stained with DAPI (*white*). *Arrow heads* indicate EdU$^+$GFP$^+$ double-positive cells. Scale bar = 50 μm.

Europe PMC Funders Author Manuscripts

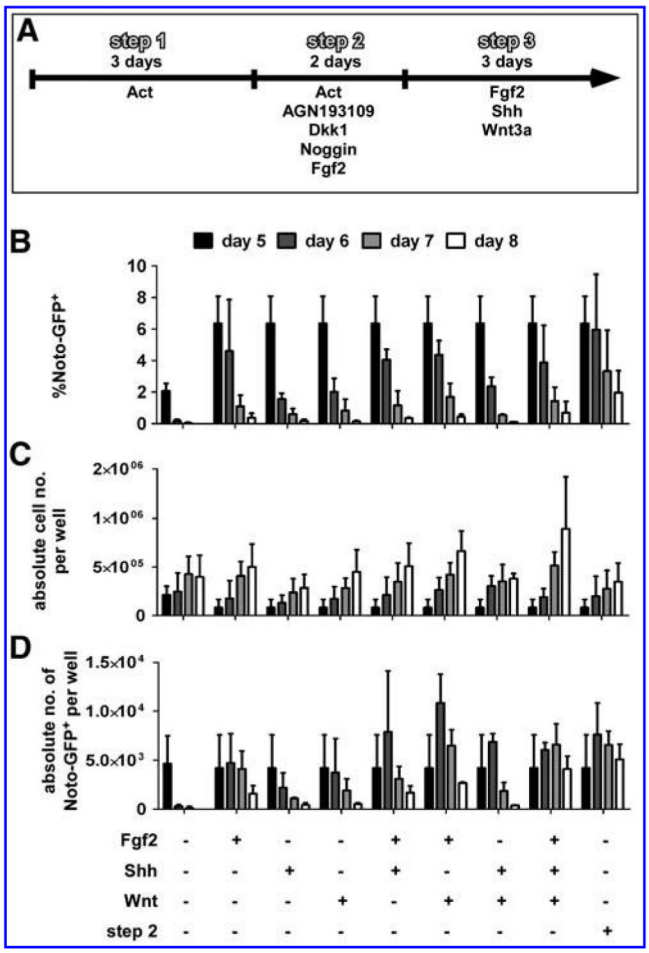

FIG. 5.

Maintenance of the Noto-GFP$^+$ cell population. Noto$^{Gfp/+}$ cells were differentiated using the 2-step differentiation protocol followed by a third step in the presence of 100 ng/mL Fgf2, 100 ng/mL Shh, or 25 ng/mL Wnt or combinations of them. Additionally, culture was continued in step 2 medium. (**A**) Schematic view of culture procedure. (**B**) FACS analysis of Noto-GFP expression was performed at day 5 to 8. (**C**) In the same setup the absolute cell number per well was counted. (**D**) Based on percentage GFP$^+$ and absolute cell number per well, the absolute number of Noto-GFP$^+$ cells per well was determined. The data represent the mean ± SD of 3 independent experiments.

Europe PMC Funders Author Manuscripts

Europe PMC Funders Author Manuscripts

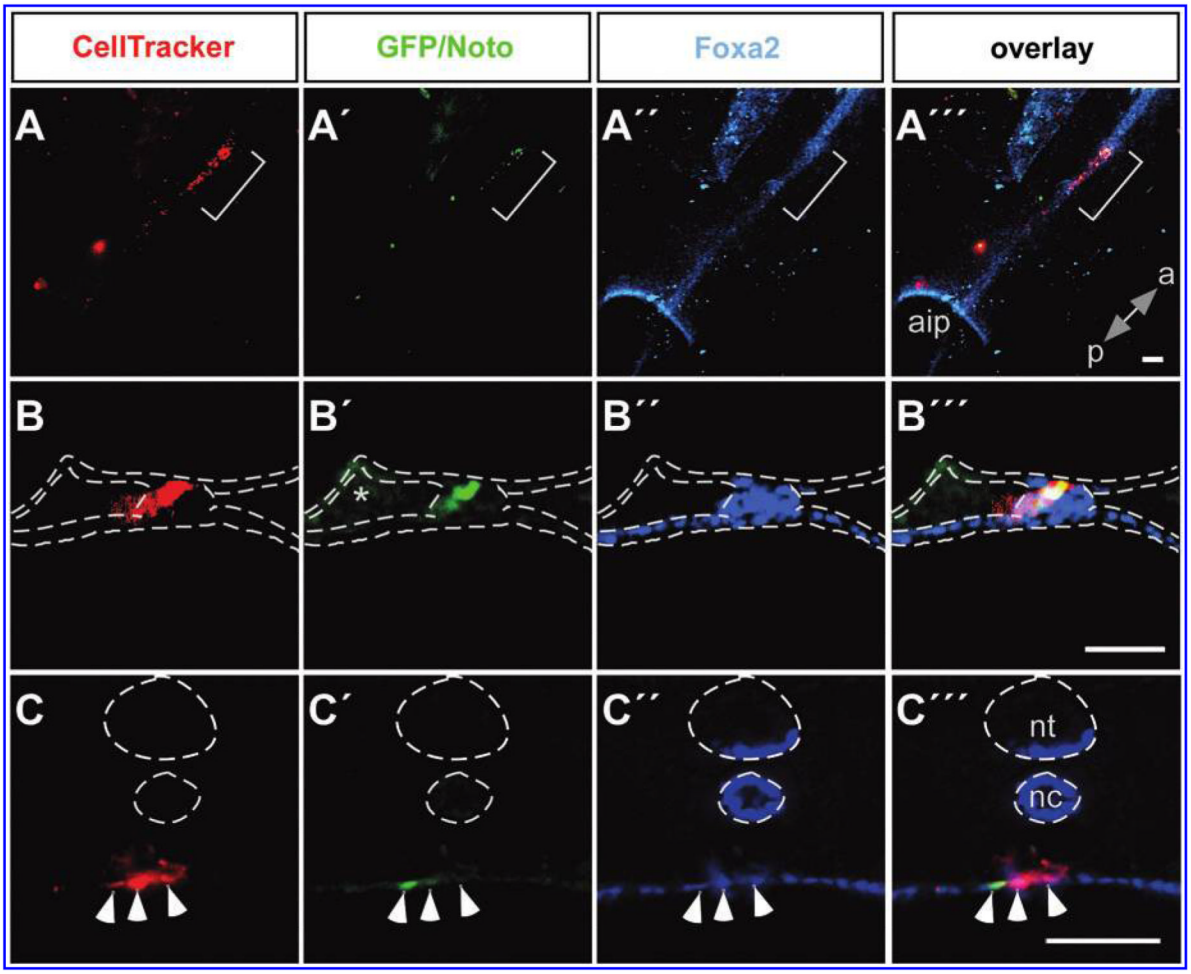

FIG. 6.

Contribution to the midline of Noto-GFP$^+$ cells grafted into chicken embryos. Noto-GFP$^+$ cells were labeled with a CellTracker™ Orange and grafted into the medial sector of the Hensen's node in HH st 4 chicken embryos (**A-C**). The chicken embryos were further cultured for 20–24 h and stained for GFP (**A′–C′**) and Foxa2 (**A″–C″**). (**A‴–C‴**) represent overlays. (**A**) Dorsal view of the midline where GFP$^+$ cells (*bracket*) have been laid down within the Foxa2$^+$ midline. (**B**) Transverse section of chicken embryos grafted at HH st 4 showing contribution of GFP$^+$ cells to the notochord or (**C**) showing contribution of grafted cells to the endoderm (*arrow heads*). All images are optical sections. a, anterior; p, posterior; aip, anterior intestinal portal; nt, neural tube; nc, notochord; *, background; scale bar = 50 μm.